R-matrix calculations of electron impact electronic excitation of BeH

2017 J. Phys. B: At. Mol. Opt. Phys. 50 175201

(http://iopscience.iop.org/0953-4075/50/17/175201)

OPEN ACCESS
IOP Publishing
Journal of Physics B: Atomic, Molecular and Optical Physics
J. Phys. B: At. Mol. Opt. Phys. **50** (2017) 175201 (12pp)
https://doi.org/10.1088/1361-6455/aa8161

R-matrix calculations of electron impact electronic excitation of BeH

Daniel Darby-Lewis[1], Zdeněk Mašín[2] and Jonathan Tennyson[1,3]

[1] Department of Physics & Astronomy, University College London,Gower St.,London, WC1E 6BT, United Kingdom
[2] Max-Born-Institut, Max-Born-Str. 2A, D-12489 Berlin, Germany

E-mail: daniel.darby.11@ucl.ac.uk, masin@mbi-berlin.de and j.tennyson@ucl.ac.uk

Received 3 March 2017, revised 6 July 2017
Accepted for publication 21 July 2017
Published 8 August 2017

Abstract

The *R*-matrix method is used to perform high-level calculations of electron collisions with beryllium mono-hydride at its equilibrium geometry with a particular emphasis on electron impact electronic excitation. Several target and scattering models are considered. The calculations were performed using (1) the UKRMol suite which relies on the use of Gaussian type orbitals (GTOs) to represent the continuum and (2) using the new UKRMol+ suite which allows the inclusion of *B*-spline type orbitals in the basis for the continuum. The final close-coupling scattering models used the UKRMol+ code and a frozen core, valence full configuration interaction, method based on a diffuse GTO atomic basis set. The calculated electronic properties of the molecule are in very good agreement with state-of-the-art electronic structure calculations. The use of the UKRMol+ suite proved critical since it allowed the use of a large *R*-matrix sphere (35 Bohr), necessary to contain the diffuse electronic states of the molecule. The corresponding calculations using UKRMol are not possible due to numerical problems associated with the combination of GTO-only continuum and a large *R*-matrix sphere. This work provides the first demonstration of the utility and numerical stability of the new UKRMol+ code. The inelastic cross sections obtained here present a significant improvement over the results of earlier studies on BeH.

Keywords: *B*-splines, fusion, *R*-matrix, BeH, electronic excitation

(Some figures may appear in colour only in the online journal)

1. Introduction

Achieving controlled and sustained nuclear fusion on Earth has been a key goal of multi-disciplinary physics for almost half a century (Winter 1975, Keilhacker *et al* 2001, Lister 2006). One of the most promising routes towards its practical implementation is using a tokamak, low density torus-shape plasma reactor, such as the Joint European Torus (JET) (Gibson 1979, Schumacher 1983). JET is conducting a vital research for the next generation of tokamaks, ITER and DEMO. Specifically the structure of JET is currently supporting an internal reactor wall called the ITER-like wall (Brezinsek *et al* 2015). This is a wall with beryllium on various plasma facing components (PFCs) as proposed for use in ITER (Kupriyanov *et al* 2015). The scrape-off layer is the plasma layer closest to the PFCs. The plasma here can interact with the reactor wall and therefore contains molecules which are formed at the wall (Federici 2006). With the addition of beryllium to the PFCs one molecule known to be formed is BeH along with its hydrogen isotope variations of deuterium (D) and tritium (T). BeH_2 is suspected to also be formed. The transport of BeH, BeD (and eventually BeT) in the JET scrape-off layer is important for tracking what happens to the tritium in the reactor, both for the future of JET and for ITER (Doerner *et al* 2007). In a plasma, with its large density of free electrons, processes involving electron collisions with BeH play

[3] Author to whom any correspondence should be addressed.

an important role in detecting and tracking the movement and deposition of BeH around the reactor (Bessenrodt-Weberpals *et al* 1987). In particular a useful diagnostic is the radiative emission coming from the A $^2\Pi \rightarrow$ X $^2\Sigma^+$ transition in BeD (Duxbury *et al* 1998, Nishijima *et al* 2008, Doerner *et al* 2009), where the initial excitation of BeD to the A-state is largely thought to originate in inelastic collisions of electrons with the molecule. There is therefore a need for accurate data on electron impact electronic excitation for applications to fusion (Samm 2005). These applications at present generally require data for BeD and will need BeT data in future.

There have been a number of recent studies on electron collisions with BeH^+ (Roos *et al* 2009, Celiberto *et al* 2012, Chakrabarti and Tennyson 2012, 2015, Laporta *et al* 2017, Niyonzima *et al* 2017), but we are only aware of a single study of electron collisional excitation of neutral BeH. This was a recent *R*-matrix calculation by Celiberto *et al* (2012). In their calculations Celiberto *et al* (2012) computed vibrationally-resolved results for electron impact electronic excitation of the molecule by combining cross sections computed using the UKRMol codes (Carr *et al* 2012) with Franck–Condon factors. These results considered only the lowest-lying electronically-excited state of BeH, the A $^2\Pi$ state, used a frozen core configuration interaction (FC-CI) model for the target wavefunctions, a small, double zeta plus polarisation basis set and *ab initio* potential energy curves (PEC) from Pitarch-Ruiz *et al* (2008).

The present paper aims to improve upon the work of Celiberto *et al* (2012) by considering many excited states, modelled using a larger basis set with diffuse orbitals. The inclusion of the diffuse basis functions is important for an accurate description of the electronic spectrum of the molecule and of the scattering observables.

The inclusion of diffuse electronic states presents a number of technical difficulties for *R*-matrix scattering calculations using the UKRMol suite which we aim to overcome here. The UKRMol suite (Carr *et al* 2012) is a well-established set of programmes for calculations of electron—molecule scattering and other processes using the *R*-matrix method (Tennyson 2010). The codes use Gaussian type orbitals (GTOs) to represent both the target and the continuum wavefunction in the region of the molecular target (Faure *et al* 2002) and employ a methodology applicable to the treatment of electronically inelastic processes (Tennyson 1996).

In practice diffuse atomic functions cannot be included in most calculations using the UKRMol suite due to numerical problems which arise when a large GTO-only continuum basis is combined with a large *R*-matrix sphere that must be used to contain the spatially extended electronic states of the target molecule (Mašín and Gorfinkiel 2011). However, this limitation has been recently overcome thanks to the newly-developed UKRMol+ suite (Mašín 2017), which allows the inclusion of *B*-spline type orbital (BTO) basis functions to represent the continuum. As we demonstrate below UKRMol+ can be used with much larger *R*-matrix spheres than UKRMol while maintaining numerical stability and quality of the continuum description.

Finally, BeH is an important molecule for testing *ab initio* methods, being the smallest, neutral open shell molecule. Therefore, much work has been done on BeH using different quantum chemical methodologies over the past 86 years (reviewed by Dattani 2015). Although similar considerations have so far not been applied to electron collision calculations we find that BeH provides a good benchmark system for such studies too.

2. Method

We use the *R*-matrix method (Tennyson 2010, Burke 2011) which spatially separates the scattering problem into an inner and an outer region. The two regions are separated by a sphere of radius $r = a$ upon which the energy-dependent *R*-matrix is constructed. In the inner region, quantum chemistry methods are used to produce full scattering energy-independent wavefunctions for the target molecule and for the target molecule plus the scattering electron. The form of the inner region wavefunction is

$$\Psi_k = \hat{A}\sum_{i,j} c_{ijk}\Phi_i^N\eta_j + \sum_m b_{mk}X_m^{N+1}. \quad (1)$$

The first of the two terms in this equation is a sum over i, j, respectively the indices for the target wavefunctions, Φ_i^N, and the continuum orbitals, η_j, where c_{ijk} is the coefficient for the ith, jth, kth term. The second term, called the L^2 term, is necessary to describe polarisation/correlation and resonance formation, this involves forming a wavefunction of the target molecule plus the scattering electrons using occupied and virtual target orbitals, the X_m^{N+1}, where b_{mk} is the coefficient for the mth, kth term.

A crucial assumption applied when selecting the target model is that the target wavefunction is entirely contained within the *R*-matrix sphere. In the outer region, the *R*-matrix is propagated to a large radius, here 100.1 a_0, then used to calculate *K*- and *T*-matrices which give scattering quantities such as eigenphases, cross-sections and resonances.

2.1. Target model

The quality of the target model depends on the quality of the atomic basis set and the level of description of electron correlation. In denoting target wavefunctions, occupancies and configurations, self consistent field molecular orbitals are used through out. The simplest *ab initio* quantum chemistry treatment in common usage is the Hartree–Fock (HF) method, in which electrons only interact with the mean averaged field of other electrons and nuclei. The corresponding HF wavefunction is represented by a single configuration. On the other end of the accuracy scale is the full configuration interaction (FCI) method, which includes all possible electron configurations constructed from all available molecular orbitals subject only to the constraints of the Pauli Principle and total symmetry, giving the best possible wavefunctions for a given basis set. Intermediate between these are the complete active space configuration interaction (CAS-CI) models where only

a subset of molecular orbitals are used in the FCI method. A special variant of the CAS-CI method is the frozen core FCI (FC-FCI) model where the atomic core orbitals are always doubly occupied and the remaining electrons are active in all the other orbitals. For BeH the FC-FCI approximation corresponds to freezing the two 1s electrons on the beryllium atom and keeping the remaining three electrons active.

The target basis sets tested here are GTO basis sets of the (aug-)cc-pV*X*Z family (Dunning 1989) where $X = $ D, T or Q (representing double zeta, triple zeta or quadruple zeta). These Dunning basis sets are designed such that the target energies converge smoothly as the size of the basis set increases. Dunning basis sets of larger size contain both larger numbers of low angular momentum Gaussians and higher angular momentum Gaussians. The 'aug-' in the above stands for augmented and means that the basis set contains additional diffuse functions, i.e. Rydberg-like orbitals.

The different basis sets have three major factors to consider in their application to these calculations. (1) Primarily the selected basis set should be able to deliver accurate energy levels (vertical excitation energies) and target properties (e.g. permanent and transition dipole moments) for all molecular states of interest. (2) The basis set should be small enough to be computationally tractable when used, in conjunction with a continuum basis, in a scattering calculation. (3) The target wavefunctions must fit inside the *R*-matrix sphere as this is the basic assumption of the method. In practice this requirement may be difficult to satisfy because diffuse functions are often necessary to accurately represent certain excited states and diffuse functions require a larger *R*-matrix sphere. The size of the *R*-matrix sphere is limited by point (2), as using a larger sphere requires greater computational resources due to the need to include many more continuum functions in the basis. In practice, if the target wavefunctions are too spatially extended and 'leak out' of the *R*-matrix sphere then problems, such as spurious resonances, can arise (Gorfinkiel *et al* 2002). Furthermore, a large target and continuum basis can also cause issues with numerical linear dependence which can manifest itself in the inner region as unphysical bound states or *R*-matrix poles.

2.2. Scattering models

The description of the scattering model involves including an additional set of orbitals to represent the continuum which must be orthogonal to the orbitals used to represent the target and the addition of the scattering electron. The simplest scattering model is the static exchange (SE) model, consisting of a HF target, $i = 1$ in equation (1) and L^2 functions from the HF target multiplied by singly occupied target virtual orbitals, $i =$ the number of virtual orbitals included. This type of calculation is only able to represent electronically elastic collisions since there is only one target state, the lack of excited states also limits the resonances that can be represented to shape resonances.

The static exchange plus polarisation (SEP) model includes all the L^2 functions generated in a SE calculation and an additional set of L^2 functions in which a single electron is excited into the the virtual orbitals along with the scattering electron. This model represents collisions where the incoming electron momentarily polarises the target molecule in the interaction but leaves it in the initial state, asymptotically, after scattering. Thanks to the inclusion of polarisation/correlation it can represent some Feshbach resonances, as well as shape resonances. Since the SEP model does not include any excited states it cannot give parent states for the Feshbach resonances and it represents only elastic scattering.

Using a CAS-CI target calculation in a scattering model is called a close-coupling (CC) scattering model. Target states are the states formed by the CAS-CI and the L^2 functions are formed by adding one more electron to the CAS. The CC-FCI method has the advantage that it allows a balanced treatment of the target and scattering problems as demonstrated in scattering calculations for few-electron targets (Stibbe and Tennyson 1997).

3. Representation of the continuum

In our calculations the continuum orbitals, see $\eta_j(\mathbf{r})$ in equation (1), are built from an additional set of continuum functions centred on the centre of mass (Faure *et al* 2002) orthogonalizing the continuum functions against the given set of target orbitals. The orthogonalization proceeds by performing first Gramm–Schmidt orthogonalization of the continuum orbitals against the set of target orbitals. In the second step the continuum orbitals are orthogonalized using the symmetric orthogonalization and those continuum orbitals with eigenvalue of the overlap matrix smaller than a given threshold are removed from the basis. The last step is crucial to maintain numerical stability of the integral calculation: continuum orbitals corresponding to eigenvalues of the overlap matrix smaller than approximately 10^{-7} contain large coefficients with alternating signs which can cause a significant precision loss (in double precision) when performing transformation of the atomic integrals to the molecular orbital basis. In other words, a careful choice of the deletion threshold is needed to prevent numerical linear dependency problems in the continuum orbital basis.

In the UKRMol suite the continuum functions are GTOs. For linear molecules there is also an option to use a Slater type orbital basis set for the target and numerically defined continuum basis set. This second option has the advantage of being usable with an arbitrarily large *R*-matrix sphere but suffers from numerical problems to do with the need to evaluate the molecular integrals numerically which leads to linear dependence difficulties with larger target basis sets. In practice recent high-accuracy studies have used the GTO option even for diatomic molecules (Little and Tennyson 2013, 2014) where the integrals over the interior of the *R*-matrix sphere can be evaluated efficiently and accurately (Morgan *et al* 1997).

However, use of GTOs to represent the continuum puts a strong upper limit on the size of the *R*-matrix sphere because increasing the radius of the sphere lowers the effective energy range for which the continuum basis is good enough

(Tarana and Tennyson 2008). This problem can be solved by adding more continuum basis functions but only up to a certain number of functions: too many continuum basis functions will cause numerical linear dependence problems within the continuum.

These limitations are best overcome substituting the radial parts of the continuum GTOs with functions more suitable for representation of the oscillating continuum wavefunction such as numerical functions with compact support. This is the approach used in the new UKRMol+ suite where the Gaussian radial part of the continuum functions is replaced with *B*-splines. As opposed to Gaussians the *B*-spline radial basis set is very flexible and does not suffer from numerical linear dependencies. The corresponding BTOs have the form:

$$\mathcal{B}(\mathbf{r})_{i,l,m} = \frac{B_i(r)}{r} X_{lm}(\Omega), \tag{2}$$

where $B_i(r)$ is the ith radial *B*-spline drawn from the set of *B*-splines which are uniquely specified by the set of knots, breakpoints and polynomial order of the *B*-splines and $X_{lm}(\Omega)$ is the real spherical harmonic. *B*-splines have been used successfully in various atomic (Zatsarinny and Bartschat 2004, Zatsarinny 2006) and molecular calculations (Sanchez and Martin 1997, Bachau *et al* 2001). However, to the best of our knowledge there is currently no application of *B*-splines to represent the continuum in molecular problems where the target molecule is represented by the standard quantum chemistry form of atom-centred GTOs.

In our approach the BTOs and the continuum GTOs can be mixed freely. This approach is useful when the set of BTOs (radial *B*-splines) is chosen to span the radial range $a_{\mathrm{GTO}} < r \leqslant a$, i.e. the radial range outside of the sphere with radius a_{GTO} up to the radius of the *R*-matrix sphere a. It is convenient to choose a_{GTO} so that all core-type GTOs and possibly the inner valence GTOs are fully contained inside it. Consequently, all mixed BTO/GTO integrals involving the product of a GTO fully contained inside the sphere $r \leqslant a_{\mathrm{GTO}}$ and a BTO are zero, thus alleviating substantially the computational demand required to calculate the mixed integrals. For small and medium-sized molecules a_{GTO} would be typically less than about 5 Bohr. In this reduced radial range, GTOs can be used to represent the continuum without linear dependency problems and to give a good representation over a wide energy range. The long distance part of the continuum wavefunction is represented by BTOs: the quality of the radial wavefunction is controlled easily by the density of the knots and the order of the *B*-splines. Finally, we note that our codes do not require the use of the continuum GTOs, i.e. in principle only BTOs can be used over the whole radial range ($a_{\mathrm{GTO}} = 0$) and vice versa the new method for continuum representation does not require the use of BTOs, i.e. the traditional GTO-only approach ($a_{\mathrm{GTO}} = a$) is still available.

Despite their attractive properties in describing the continuum, the use of numerical functions leads to the problem of performing an efficient and accurate calculation of the multicentric molecular integrals involving the numerical function and the GTOs. An approach combining the use of a finite element method—discrete variable representation (FEM-DVR) for the continuum and atom-centred GTOs has been used successfully for small molecules in the photo-ionisation calculations of Yip *et al* (2014). Legendre expansion of the Coulomb potential and Lebedev numerical quadrature were used to calculate required molecular integrals for one and two particles in the continuum.

Our approach to the mixed-integral evaluation does not require the use of the numerical (Lebedev) angular quadrature and relies instead on analytic form of certain intermediate integrals. However, we retain the use of the Legendre expansion for calculation of the mixed exchange integral. The details of the integral evaluation will be described in detail in subsequent publications.

3.1. Structure of the codes

The calculation of both GTO-only and the mixed BTO/GTO molecular integrals has been implemented in a new integral library (Mašín 2017). The new code replaces completely the original GTO integral core of the inner region part of the UKRMol suite (programmes SWMOL3, SWORD, SWTRMO, GAUSPROP, SWEDMOS). The calculation of the atomic integrals, generation of the continuum orbitals and the integral transformation are all carried out at once using a parallelised integral library. The integral calculation requires on input a set of molecular orbitals saved in the MOLDEN format (Schaftenaar and Noordik 2000) which can be obtained using a range of quantum chemistry software. The integrals, atomic and molecular basis sets are saved in a single file and accessed by the standard UKRMol programmes which perform the Hamiltonian construction and diagonalisation (SCATCI), calculation of the target properties (DENPROP) and the construction of the *R*-matrix amplitudes (SWINTERF). An interface to the CDENPROP programme used for photoionization calculations has been implemented too but not used as part of the work presented here. The new integral library and the set of UKRMol programmes adapted to it form the UKRMol+ suite of codes.

The polyatomic codes UKRMol and UKRMol+, in common with most quantum chemistry codes, cannot use full linear symmetry. All calculations presented here were therefore performed in C_{2v}; C_{2v}-symmetry notation is used when discussing input to the codes but all final results, except for eigenphases, are transformed to the full ($C_{\infty v}$) symmetry notation which is straightforward to achieve.

4. Results

4.1. Target model comparisons

The target model selection was based upon the premise of getting the most accurate target energies and dipole moments within the allowed computational and *R*-matrix radius constraints. To select the optimal model we test the use of different atomic basis sets in combination with the FCI and FC-FCI methods. We also test a smaller CAS-CI

Table 1. GS energy (in Hartree), vertical excitation energies (in eV), permanent dipole moment for the ground state (in au) and the magnitudes of the transition dipole moments for the initial ground state (in au) as calculated in this work and compared with reference experimental and theoretical values. Question marks on state assignments show that the given experimental state assignments are uncertain.

GS energy and excitation energies

			CAS-CI	Full CI	Frozen core full CI			
State	Experimental[a]	Literature[b]	cc-pVDZ	cc-pVDZ	cc-pVDZ	aug-cc-pVDZ	cc-pVTZ	aug-cc-pVTZ
X $^2\Sigma^+$		−15.194	−15.173	−15.189	−15.188	−15.190	−15.196	−15.197
1 (A) $^2\Pi$	2.48	2.500	2.481	2.554	2.557	2.524	2.519	2.500
2 $^2\Sigma^+$		5.539	5.614	5.690	5.695	5.530	5.696	5.521
3 (C) $^2\Sigma^+$	3.84	5.532	7.617	7.647	7.649	5.633	6.812	5.646
1 $^4\Pi$		5.770	5.609	5.796	5.799	5.753	5.852	5.821
4 $^2\Sigma^+$	6.06	6.107	8.989	9.055	9.054	6.233	7.202	6.226
2 (B) $^2\Pi$	6.31	6.313	7.472	7.582	7.592	6.435	7.564	6.465
5 $^2\Sigma^+$		6.706	10.059	10.221	10.227	7.450	9.077	7.219
3 (D?) $^2\Pi$	6.71	6.712	7.948	8.100	8.109	7.366	7.905	7.316
6 (E) $^2\Sigma^+$	6.71	7.019	10.876	10.992	10.998	7.645	10.391	7.420
4 (G) $^2\Pi$	7.28	7.352	9.860	9.933	9.936	7.814	8.434	7.766
1 (D?) $^2\Delta$	6.74	6.747	9.039	9.255	9.261	8.290	9.109	7.942
5 $^2\Pi$		7.266	13.468	13.632	13.636	8.576	12.147	8.165

Permanent dipole moment for the ground state

		CAS-CI	Full CI	Frozen core full CI			
State	Literature[b,c]	cc-pVDZ	cc-pVDZ	cc-pVDZ	aug-cc-pVDZ	cc-pVTZ	aug-cc-pVTZ
X $^2\Sigma^+$	0.065 (0.0561)	0.003	0.061	0.060	0.095	0.070	0.090

Transition dipole moments for the initial ground state

		CAS-CI	Full CI	Frozen core full CI			
State	Literature[b]	cc-pVDZ	cc-pVDZ	cc-pVDZ	aug-cc-pVDZ	cc-pVTZ	aug-cc-pVTZ
1 (A) $^2\Pi$	0.871	0.812	0.840	0.840	0.859	0.857	0.865
2 $^2\Sigma^+$	0.612	0.352	0.303	0.302	0.577	0.291	0.595
3 (C) $^2\Sigma^+$	0.188	1.051	1.077	1.078	0.207	0.051	0.101
4 $^2\Sigma^+$	0.594	0.772	0.732	0.729	0.369	1.152	0.443
2 (B) $^2\Pi$	0.390	0.819	0.917	0.917	0.212	0.879	0.246
5 $^2\Sigma^+$	0.757	0.525	0.560	0.563	1.327	1.003	1.380
3 (D?) $^2\Pi$	0.417	1.086	0.957	0.961	0.720	0.961	0.733
6 (E) $^2\Sigma^+$	0.207	0.466	0.430	0.428	0.540	0.051	0.109
4 (G) $^2\Pi$	0.307	0.251	0.244	0.240	1.015	0.135	0.979
5 $^2\Pi$	0.342	0.164	0.166	0.065	0.935	0.184	0.907

[a] Collected experimental adiabatic excitation energies taken from Pitarch-Ruiz *et al* (2007).
[b] Theoretical results of Pitarch-Ruiz *et al* (2007, 2008).
[c] The value in braces is from calculations by Celiberto *et al* (2012).

model in which the two core electrons on Be are frozen and three electrons occupy a smaller set of $8a_1$, $3b_1$, $3b_2$ and $1a_2$ molecular orbitals. Due to the factorial scaling of the CI methods the computational demands significantly increase when going from three (i.e. frozen core) to five (i.e. all) active electrons and from the double zeta (pVDZ) to triple zeta (pVTZ) basis sets.

While some tests were performed for our target wavefunctions over a range of bond-lengths, all calculations presented here were performed in the centre-of-mass frame at the experimental equilibrium bond-length of $R = 1.3426$ Å (Huber and Herzberg 1979). The target calculations were performed using HF orbitals generated using MOLPRO (Werner *et al* 2008).

Table 1 shows the calculated ground state (GS) energy, in Hartree, vertical electronic excitation energies, in eV, and the dipole moments for the various models tested by us and in comparison with the high accuracy electronic structure calculations of Pitarch-Ruiz *et al* (2007) and the available experimental values of adiabatic excitation energies. The state labels and the experimental values have been taken from Pitarch-Ruiz *et al* (2007). We note that Pitarch-Ruiz *et al* (2007) used a slightly different value for the bond length (1.326 903 Å) in their single geometry calculations but, this difference has only a minimal effect on the calculated values. Nonetheless energies in table 1 are taken from PECs from Pitarch-Ruiz *et al* (2008). According to Pitarch-Ruiz *et al* (2007) the adiabatic nature of the experimental energies

compared to the vertical nature of theoretical energies is the most important factor explaining the sometimes significant differences between their calculated and the experimental values, like the large difference between these values for the C-state. Excluding the C-state the agreement of their calculated data with experiment is very good and therefore in the following we use the calculated values of Pitarch-Ruiz *et al* (2007) as an accurate reference for our calculations.

Comparing our results obtained using the cc-pVDZ basis set and the three different models for electron correlation, we observe only negligible differences between the FCI and the FC-FCI results for both the vertical excitation energies and the dipole moments. We conclude that the frozen core approximation leads to an insignificant loss of accuracy, especially for the low-lying states, compared to the five-electron FCI calculation, despite a very significant reduction in computational cost. The differences between the FC-FCI model and the CAS-CI model are mostly small but non-negligible making the FC-FCI model preferable.

The vertical excitation energies obtained using the FC-FCI (cc-pVDZ) model are in good agreement (within 0.2 eV) with the reference values only for the states 1 (A) $^2\Pi$, 2 $^2\Sigma^+$ and 1 $^4\Pi$ which are all valence states while most of the remaining states have a Rydberg character (Pitarch-Ruiz *et al* 2007). These results suggest that the main deficiency of this model is the absence of diffuse functions in the atomic basis. Indeed, as seen from the table the use of the cc-pVTZ basis which is larger than cc-pVDZ but does not include diffuse functions does not lead to a good agreement between ours and the reference values for the diffuse states. The agreement with the reference values is dramatically improved when the FC-FCI method together with the augmented (diffuse) basis sets is used: the agreement is excellent (within 0.12 eV) for the lowest six excited states. The differences between the aug-cc-pVDZ and aug-cc-pVTZ are mostly negligible but the FC-FCI model using the aug-cc-pVDZ basis is computationally significantly cheaper than the one using the aug-cc-pVTZ basis. We also tested the use of the aug-cc-pVQZ basis set (not shown) but found little improvement over the aug-cc-pVTZ results with respect to the increase in computational cost.

Table 1 includes the dipole transition moments between the ground state and the excited states and the value of the permanent dipole moment for the ground state obtained using the different target models. The magnitude of the permanent dipole moment is small (subcritical) but, as we will see below, its variation between the different target models has a significant influence on the corresponding elastic scattering cross sections. The comparison of the dipole transition moments for the FC-FCI (aug-cc-pVDZ) model with the reference values shows larger differences in comparison with the vertical energies but that is to be expected since dipole moments are generally the more sensitive property. Nevertheless, the agreement with the reference values for the first six states is still good. We conclude that the FC-FCI model using the aug-cc-pVDZ atomic basis is optimal in terms of accuracy and computational cost. This will be our preferred model for use in the scattering calculations.

4.2. Scattering models for GTO-only UKRMol calculations

The calculations using the GTO-only representation of the continuum were performed using the UKRMol suite. We found that the scattering calculations using our preferred target model FC-FCI (aug-cc-pVDZ) were not possible due to the limits on the size of the *R*-matrix sphere and the diffuse character of the target states resp. target orbitals. To avoid these problems we have used the compact cc-pVDZ atomic basis set and *R*-matrix radius $a = 14$ Bohr. The exponents of the continuum GTOs were optimised according to the methods of Faure *et al* (2002) and for angular momentum up to $l = 4$. The deletion threshold used in the symmetric orthogonalization was set to 2×10^{-7}.

We have found that even with the compact atomic basis we could not include all target molecular orbitals in the calculation: some virtual orbitals were too spatially extended to be contained within the *R*-matrix sphere. To illustrate this point we show in figure 1 eigenphase sums for the $^3A_1$ and $^3B_{1/2}$ scattering symmetries obtained from three different models: the SE model using all virtuals (SE-AV), the SE model using a reduced set of virtuals (SE-RV) and the CAS-CI model using the reduced set of virtuals and all 21 target states lying below 11 eV (CAS-CI). The SE calculations are not able to describe electronically inelastic processes and therefore have only a limited validity for electron energies larger than the threshold for the first electronically excited state (≈2.5 eV). The CAS-CI calculations are reliable up to the ionisation threshold (≈8.2 eV), the results beyond this energy must be interpreted with care.

The calculations using the SE-AV model included the HF wavefunction to represent the ground state of the molecule and all virtual orbitals available ($10a_1$, $4b_1$, $4b_2$ and $1a_2$) coupled to it to represent the L^2 functions in the scattering model, see equation (1) above. The eigenphase sum for the $^3B_{1/2}$ symmetry displays a broad jump of π around 1 eV which is a signature of a shape resonance—the only type of resonance the SE model can represent. The eigenphase sum for the $^3A_1$ symmetry displays a sharp jump around 1 eV and a broader one around 8 eV. In the SE-RV model the number of virtual orbitals used is decreased to $8a_1$, $3b_1$, $3b_2$ and $1a_2$ and both of these structures in the $^3A_1$ symmetry disappear, confirming they are unphysical. This problem is typical for calculations in which some of the target orbitals are not fully contained by the *R*-matrix sphere. Increasing the size of the *R*-matrix sphere beyond 14 Bohr is possible but only at the expense of reducing the energy range for the scattering electron. For the present case of $a = 14$ Bohr the continuum basis set is accurate up to scattering energy of approximately 15 eV but increasing the radius to 16 Bohr makes the valid energy range drop to below 10 eV. To the best of our knowledge the largest radius used in any GTO-based *R*-matrix scattering calculation was the calculation of Tarana *et al* (2009) on Li_2 where radius of 22 Bohr was used but the electron energy range was limited to energies below approx. 2.5 eV.

The results for the CAS-CI model using the reduced set of virtuals and 21 target states represent the highest-level results obtained in this work using the UKRMol code. The

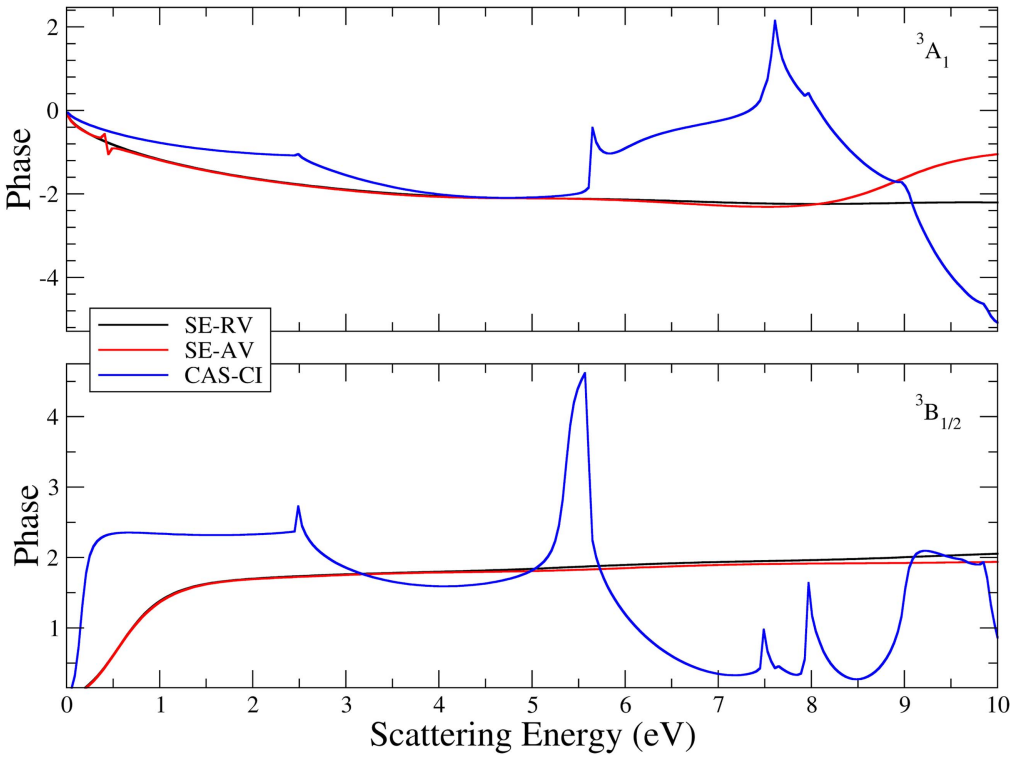

Figure 1. Eigenphase sums for the $^3A_1$ and $^3B_{1/2}$ symmetries calculated using UKRMol and various scattering models: static exchange using all virtuals (SE-AV), static exchange using a reduced set of virtuals (SE-RV) and complete active space CI (CAS-CI).

eigenphase sums for this model clearly show a number of resonances which we further discuss below. Here we only note the importance of modelling polarisation/correlation for accurate description of the lowest-lying resonance in the $^3B_{1/2}$ symmetry which appears much lower in energy and has a smaller width in the CAS-CI results compared with the SE-AV results.

Although a CAS-CI calculation with the cc-pVTZ atomic basis is computationally tractable it has worse issues with linear dependence and functions leaking outside of the sphere. The increase in accuracy potentially achievable from the increase from cc-pVDZ to cc-pVTZ, as discussed in the preceding section, is also not significant in comparison to the increase in computational cost.

4.3. Scattering models for GTO/BTO UKRMol+ calculations

The calculations performed using UKRMol+ and the mixed GTO/BTO basis for the continuum were not limited by the size of the *R*-matrix sphere, a crucial advantage over UKRMol. Here we present only the results obtained using the preferred model FC-FCI (aug-cc-pVDZ) but calculations were performed using the simpler UKRMol models to verify correctness of the new code. The close-coupling calculations included all electronic states below 12 eV, 50 states in total. We have found that to confine them sufficiently a large radius of 35 Bohr was needed. This was achieved using a mixed basis for the continuum composed of a small set of continuum GTOs with exponents showed in table 2 and a basis of BTOs built from a basis of radial *B*-splines spanning the radial range from $a_{GTO} = 3.5$ Bohr to the *R*-matrix sphere. Continuum angular momenta up to $l = 6$ were included in the calculation. The basis of continuum GTOs was optimised using NUMCBAS and GTOBAS (Faure *et al* 2002) for a small radius of 4 Bohr. The basis of radial *B*-splines comprised 20 functions of order 9 but the first two had to be removed from the calculation since they do not have smooth first derivative at the starting point $r = 3.5$ Bohr. Since the linear dependency problems are mitigated when BTOs are used the deletion threshold for orthogonalization was set to 10^{-5}, a value much larger than in the UKRMol calculations, while removing only a few continuum orbitals per symmetry from the basis. With these parameters the continuum basis was accurate for electron energies up to approx. 15 eV. Table 3 shows a summary of the issues with the trialed target and scattering models.

Table 2. Exponents of the continuum GTOs for partial waves up to $l = 6$ optimised for radius of 4 Bohr.

l	Exponents			
0	0.601 8850	0.251 7630	0.099 7470	0.035 5189
1	0.627 9660	0.302 6600	0.139 2060	0.057 5246
2	0.430 0720	0.204 6800	0.089 1347	
3	0.474 4870	0.237 3500	0.108 8240	
4	0.311 8840	0.135 3390		
5	0.348 4640	0.157 7080		
6	0.384 7250	0.179 8360		

Table 3. Comparison of issues with scattering results for various models and basis sets calculated with UKRMol and UKRMol+.

Model	Scattering wavefunction	Target model	UKRMol comments	UKRMol+ comments
SE	Reduced virtual	{HF cc-pVDZ HF aug-cc-pVDZ HF cc-pVTZ}	{HF target model, well behaved}.	{Unchanged}.
	All virtual	{HF cc-pVDZ HF aug-cc-pVDZ HF cc-pVTZ}	{HF target model, functions outside box, linear dependence and spurious resonances}.	{HF target model, box size and linear dependence issues removed}.
SEP	Converged virtual	HF cc-pVTZ	{HF target model and only limited resonances found}.	{Unchanged}.
CC CAS-CI	{Converged virtual, frozen core}	CAS-CI cc-pVDZ	{Poor target model}.	{Unchanged}.
		CAS-CI aug-cc-pVDZ	{Functions outside box}.	{Box size issues removed}.
		CAS-CI cc-pVTZ	{Poor target model}.	{Unchanged}.
CC FC-FCI	{All virtual, frozen core}	FC-FCI cc-pVDZ	{Poor target model and linear dependence}.	{Poor target model, linear dependence issues removed}.
		FC-FCI aug-cc-pVDZ	{Accurate target model, functions outside box and linear dependence}.	{Accurate target model, box size and linear dependence issues removed}.
		FC-FCI cc-pVTZ	{Poor target model, functions outside box, linear dependence and computationally untractable}.	{Poor target model and computationally untractable, box size and linear dependence issues removed}.
CC-FCI	{All virtual, active core}	FCI cc-pVDZ	{Poor target model and linear dependence}.	{Poor target model, linear dependence issues removed}.
		FCI aug-cc-pVDZ	{Accurate target model, functions outside box, linear dependence and computationally untractable}.	{Accurate target model, box size and linear dependence issues removed, severely computationally untractable}.
		FCI cc-pVTZ	{Poor target model and severely computationally untractable}.	{Unchanged}.

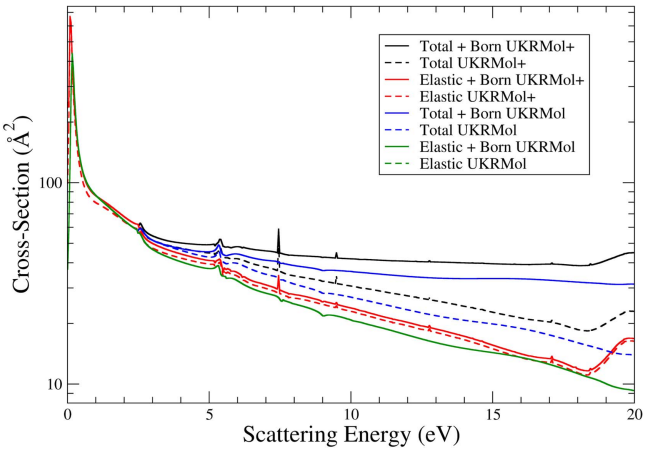

Figure 2. Total and elastic cross-sections for the ground state calculated using the UKRMol and UKRMol+ codes. The cross-sections including the Born correction are plotted using solid lines.

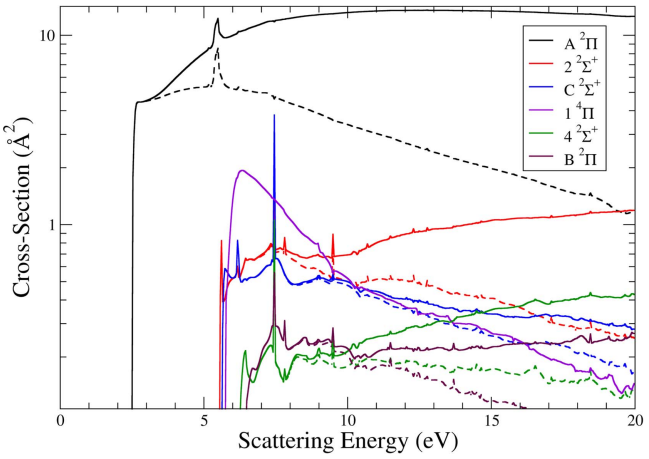

Figure 3. Electron impact electronic excitation cross-sections for the ground initial state (X $^2\Sigma^+$) and the six lowest lying final electronic states calculated using UKRMol+. The cross-sections including (excluding) the Born correction are plotted in solid (dashed) lines.

4.4. Final scattering results

In figure 2 we show the elastic and total scattering cross sections for the ground electronic state. Results of several calculations are shown: the UKRMol calculations were performed using the CAS-CI (cc-pVDZ) model while the UKRMol+ calculations employed the FC-FCI (aug-cc-pVDZ) model. Since the BeH molecule has a permanent dipole moment the long range interaction of the dipole with the continuum electron causes a slow convergence of the partial wave expansion for the continuum wavefunction. We estimate the contribution of partial waves beyond $l = 4$ (UKRMol) and $l = 6$ (UKRMol+) using the Born correction for the rotating dipole as implemented in BORNCROS Norcross and Padial (1982). The corresponding Born-corrected total and elastic cross sections are plotted using solid lines, the total Born correction include the elastic and inelastic born corrections as well.

Comparing first the elastic cross-sections obtained using UKRMol (green) and UKRMol+ (red) we see that the latter is larger which can be explained mainly by the larger dipole moment of the ground state in the FC-FCI model (0.095 au) compared with the CAS-CI value (0.003 au). The small magnitude of the CAS-CI permanent dipole is also reflected in a very small contribution of the Born correction making the *ab initio* (solid green line) and the Born-corrected cross sections (dashed green line) indistinguishable in the plot. However, the UKRMol and UKRMol+ cross sections have a similar shape and show the same resonant peaks with exception of a few more narrow peaks appearing in the UKRMol+ results, discussed below.

The total cross sections (blue UKRMol, black UKRMol+) are much larger than the elastic ones for energies beyond the first excited state highlighting the importance of inelastic processes for electron collisions with BeH. We also observe the significant difference between the magnitudes of the UKRMol and UKRMol+ total cross sections at higher energies which is not explained by the difference in the elastic cross sections

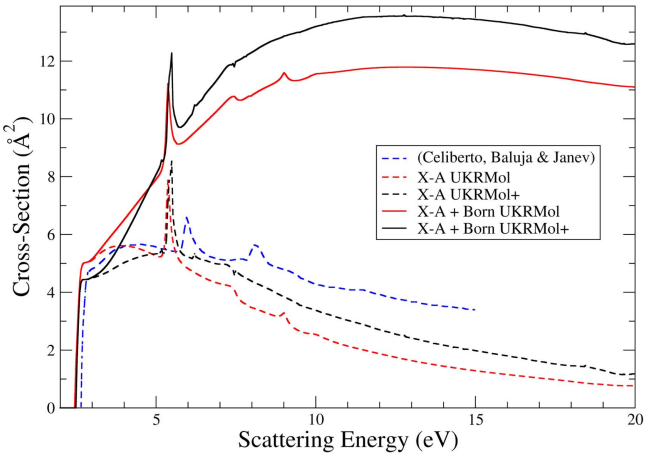

Figure 4. Comparison of electron impact electronic excitation cross-sections from the ground state, X $^2\Sigma^+$, to the lowest lying excited state, A $^2\Pi$. Solid lines are the cross-sections including the Born correction. Dashed blue line is the *R*-matrix result from Celiberto *et al* (2012).

alone and points to the importance of using a highly accurate model to describe electronically inelastic processes.

Figure 3 is a log plot of the UKRMol+ cross-sections for electron impact electronic excitation from the ground state to the first six excited states. In solid lines are inelastic cross-sections including the Born correction calculated using the approach of Norcross and Padial (1982). The Born correction was calculated for all dipole allowed transitions from the ground state, i.e. excluding the spin-forbidden transition to the 1 $^4\Pi$ state. We can see that the Born correction makes a very significant contribution to the cross section for excitation of some of the states, e.g. the first excited state 1 (A) $^2\Pi$ and reflects the magnitudes of the corresponding transition dipole moments listed in table 1.

Figure 4 compares our cross sections for impact excitation of the A-state with the one calculated by Celiberto *et al* (2012). The blue line is the *R*-matrix cross-section from

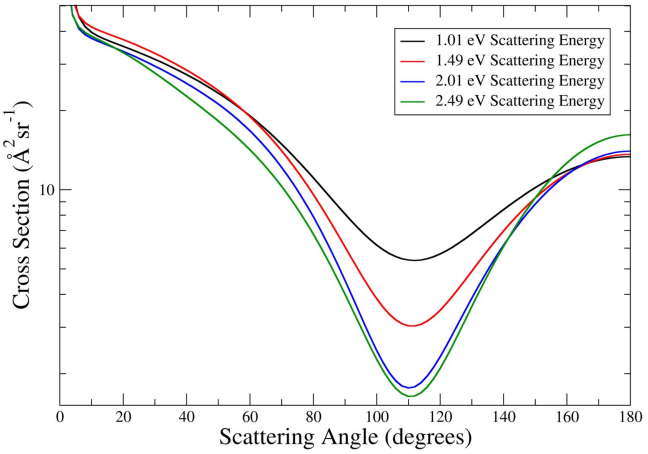

Figure 5. Differential cross-sections of from the UKRMol+ final model. The peak values are 1.68×10^6 Å^2 sr^{-1}, 3.01×10^6 Å^2 sr^{-1}, 4.73×10^6 Å^2 sr^{-1} and 6.52×10^6 Å^2 sr^{-1} at scattering energies of 1.01 eV, 1.49 eV, 2.01 eV and 2.49 eV, respectively.

figure 4 of the paper by Celiberto *et al* (2012). The lines in black are results from the final model of UKRMol+ and in red are the results from the final model of UKRMol. The results in dashed lines are without the Born correction and the solid lines are results with the Born correction added. We observe that above about 8 eV our uncorrected cross sections are significantly smaller than those of Celiberto *et al* (2012) and that the resonances in our calculations are found at lower energies and have smaller widths. This is consistent with our target and scattering models being larger and more accurate at describing polarisation/correlation effects.

Figure 4 also shows the importance of the Born correction: at 10 eV the Born-corrected results are approximately a factor of three to four larger than the corresponding uncorrected results. This finding can be put in contrast with the results of Celiberto *et al* (2012). They calculate the impact cross section in the Born approximation, which includes contributions of all partial waves, and compare it to their *ab initio* result which includes partial waves only up to $l = 4$ and to a result of the modified Mott–Massey approximation (TM MM) scaled down to match the *R*-matrix result. The scaled TM MM results are then used to estimate the cross section for very large electron energies up to 1000 eV. However, since the Born correction is large, scaling the TM MM result to a cross section not including it causes a significant underestimation of the TM MM results for the whole energy range.

Figure 5 shows sample differential cross sections, calculated using POLYDCS (Sanna and Gianturco 1998) for scattering energies of 1.01, 1.49, 2.01 and 2.49 eV. As would be expected for a dipolar system, the cross sections are largest at 0°, where the cross sections are all in the order of 10^6 Å^2 sr^{-1} in comparison to the magnitude of 10^1 Å^2 sr^{-1} at higher angles.

Electron resonances can influence cross sections for a range of processes including impact excitation. This can be seen, for example, in figure 4 where the most prominent peak at around 5.2 eV is caused by a resonance. Table 4 collects the resonances and their parameters found in our results by fitting the eigenphase sums to the Breit–Wigner form. The table compares the resonance parameters as obtained using the cc-pVDZ atomic basis and UKRMol suite with the results of the FC-FCI (aug-cc-pVDZ) model and UKRMol+ suite. We find a single narrow shape resonance of $^3\Pi$ symmetry close to the threshold. This is also the only resonance that can be described by the SE (HF) model. We have used the SE plus polarisation (SEP) method (not shown) to see if more shape resonances are present but no additional resonances are found. The close-coupling models reveal the formation of a number of resonances of core-excited character.

The parent state, 1 (A) $^2\Pi$, with the main configuration $1\sigma^2 2\sigma^2 1\pi$ might be expected to support three resonances with the configuration $1\sigma^2 2\sigma^2 1\pi^2$. Resonances with $^1\Delta$ symmetry at ≈2.6 eV, and $^1\Sigma^+$ symmetry at ≈5.2 eV can clearly be seen. However, the expected, lower-lying resonance of $^3\Sigma^-$ symmetry is not observed. This is because this state lies below the 1 (A) $^2\Pi$ target parent state, and there is no allowed decay route to the GS. The $^3\Sigma^-$ states therefore forms a bound state in the continuum or a resonance with infinitesimal width (Stillinger and Herrick 1975).

The most prominent resonance from figure 4, the $^3\Pi$ at ≈5.5 eV, lies about 8% lower in energy in our work from UKRMol than in the work of Celiberto *et al* (2012). There is also an uncertainty between our UKRMol and UKRMol+ models of about 2% for the positions of this resonance and an average difference in the position of resonances of ±30 meV.

5. Conclusions

We have performed *R*-matrix calculations of elastic and inelastic electron collisions with BeH using scattering models ranging from SE to FCI. This work is the first application of the new set of UKRMol+ *R*-matrix codes which use a mixed *B*-spline/Gaussian basis for the continuum. The new suite has allowed us to use a large R-matrix radius of 35 Bohr without compromising the quality of the continuum description thus enabling the use of a diffuse atomic basis to represent accurately electronic states of the target molecule. The vertical excitation energies and the properties of the low-lying electronic states (up to 6.5 eV) are in an excellent agreement with experiment and high-level electronic structure calculations. A careful comparison of the scattering results obtained with the new UKRMol+ and the old UKRMol codes has been done to verify the validity and accuracy of the new code.

FCI models have been used to calculate elastic and electron impact electronic excitation cross sections using more accurate models than in the previous studies. This includes a correct treatment of the Born correction for the inelastic cross section. We demonstrate the importance of the Born correction for this system and in particular for the cross section for electron impact excitation of the lowest-lying excited state A $^2\Pi$. It is radiative emissions from this state that have been observed in fusion plasmas and we find that this cross section was significantly underestimated in the only previous *R*-matrix study. Finally, we find and characterise

Table 4. Resonances found using the various scattering models employing UKRMol (SE, SEP, CC CAS-CI) and UKRMol+ (CC FC-FCI). Resonance positions and widths (in brackets) are in eV. Tentative resonance classifications and associated configurations are also given.

	SE	SEP	CC CAS-CI	CC FC-FCI	Resonance classification	
$^3\Pi$	0.572 [0.909]	0.235 [0.204]	0.155 [0.126]	0.090 [0.092]	$[1\sigma^2 2\sigma^2 3\sigma^1 1\pi^1]$	Shape
$^1\Delta$			2.572 [0.352]	2.55 [0.2][a]	$[1\sigma^2 2\sigma^2 1\pi^2]$	Core excited
$^1\Sigma^+$			5.63 [0.05][a]	5.195 [0.024]	$[1\sigma^2 2\sigma^2 1\pi^2]$	Core excited
$^3\Sigma^+$			5.64 [0.04][a]	5.366 [0.008]	$[1\sigma^2 2\sigma^2 4\sigma^1 5\sigma^1]$	Feshbach
$^3\Pi$			5.364 [0.142]	5.487 [0.017]	$[1\sigma^2 2\sigma^2 1\pi^1 4\sigma^1]$	Feshbach
$^3\Sigma^-$			5.810 [0.943]	5.8 [0.9][a]	$[1\sigma^2 2\sigma^1 3\sigma^1 1\pi^2]$	Core excited

[a] Estimated, not fitted.

several electron resonances which appear below 8 eV and enhance both the elastic and inelastic cross sections.

This work is an important step forward in providing high accuracy theoretical data necessary in fusion applications, especially that required by modellers at JET. For this it will be necessary to consider separately BeH, BeD and BeT; these isotopologues can be distinguished from each other through the treatment of nuclear motion which requires calculations at different geometries. These geometry resolved *R*-matrix data are currently being computed. Once completed these collision data will be combined with high accuracy line lists generated from PECs with coupling terms and Born–Oppenheimer breakdown effects which have been calculated for BeH, BeD and BeT (Darby-Lewis *et al* 2017). The line lists, in combination with transition rates from the geometry resolved *R*-matrix results, and a collisional radiative model will be used to generate non-Boltzmann populations of states and highly precise spectra for each isotopologue. This will be compared to current high resolution spectra of BeH and BeD from JET, and future BeT spectra.

Acknowledgments

We would like to thank the Engineering and Physical Sciences Research Council (EPSRC) for studentship (EP/M507970/1) and the Culham Centre for Fusion Energy (CCFE) for funding. We would also like to thank the people and groups who have worked on the UKRMol and UKRMol+ suites. ZM gratefully acknowledges collaboration with Jimena Gorfinkiel, Agnieszka Sieradzka, Alex Harvey and Danilo Brambila on the development and testing of the UKRMol+ suite of codes.

ORCID iDs

Jonathan Tennyson https://orcid.org/0000-0002-4994-5238

References

Bachau H, Cormier E, Decleva P, Hansen J E and Martin F 2001 *Rep. Prog. Phys.* **64** 1815–1943
Bessenrodt-Weberpals M, Hackmann J and Uhlenbusch J 1987 *J. Nucl. Mater.* **145** 849–53
Brezinsek S *et al* 2015 *Nucl. Fusion* **55** 063021
Burke P G 2011 *R-Matrix Theory of Atomic Collisions: Application to Atomic, Molecular and Optical Processes* (Berlin: Springer)
Carr J M, Galiatsatos P G, Gorfinkiel J D, Harvey A G, Lysaght M A, Madden D, Mašín Z, Plummer M and Tennyson J 2012 *Eur. Phys. J.* D **66** 58
Celiberto R, Baluja K L and Janev R K 2012 *Plasma Sources Sci. Technol.* **22** 015008
Celiberto R, Janev R and Reiter D 2012 *Plasma Phys. Control. Fusion* **54** 035012
Chakrabarti K and Tennyson J 2012 *Eur. Phys. J.* D **66** 31
Chakrabarti K and Tennyson J 2015 *J. Phys. B: At. Mol. Opt. Phys.* **48** 235202
Darby-Lewis D, Tennyson J, Lawson K D, Stamp M F and Shaw A 2017 *J. Phys. B: At. Mol. Opt. Phys.* submitted
Dattani N S 2015 *J. Mol. Spectrosc.* **311** 76–83
Doerner R, Baldwin M, Hanna J, Linsmeier C, Nishijima D, Pugno R, Roth J, Schmid K and Wiltner A 2007 *Phys. Scr.* **T128** 115
Doerner R P, Baldwin M J, Buchenauer D, De Temmerman G and Nishijima D 2009 *J. Nucl. Mater.* **390–91** 681–4
Dunning T 1989 *J. Chem. Phys.* **90** 1007–23
Duxbury G, Stamp M F and Summers H P 1998 *Plasma Phys. Control. Fusion* **40** 361–70
Faure A, Gorfinkiel J D, Morgan L A and Tennyson J 2002 *Comput. Phys. Comm.* **144** 224–41
Federici G 2006 *Phys. Scr.* **T124** 1
Gibson A 1979 *Naturwissenschaften* **66** 481–8
Gorfinkiel J D, Morgan L A and Tennyson J 2002 *J. Phys. B: At. Mol. Opt. Phys.* **35** 543–55
Huber K P and Herzberg G 1979 *Molecular Spectra and Molecular Structure IV. Constants of Diatomic Molecules* (New York: Van Nostrand-Reinhold)
Keilhacker M, Gibson A, Gormezano C and Rebut P 2001 *Nucl. Fusion* **41** 1925
Kupriyanov I B, Nikolaev G N, Kurbatova L A, Porezanov N P, Podkovyrov V L, Muzichenko A D, Zhitlukhin A M, Gervash A A and Safronov V M 2015 *J. Nucl. Mater.* **463** 781–6
Laporta V, Chakrabarti K, Celiberto R, Janev R K, Mezei J Z, Niyonzima S, Tennyson J and Schneider I 2017 *Plasma Phys. Control. Fusion* **59** 045008
Lister J 2006 *Fusion: The Energy of the Universe* (Bristol: IOP Publishing)
Little D A and Tennyson J 2013 *J. Phys. B: At. Mol. Opt. Phys.* **46** 145102
Little D A and Tennyson J 2014 *J. Phys. B: At. Mol. Opt. Phys.* **47** 105204
Mašín Z 2017 The UKRMol. codes in preparation
Mašín Z and Gorfinkiel J D 2011 *J. Chem. Phys.* **135** 144308
Morgan L A, Gillan C J, Tennyson J and Chen X 1997 *J. Phys. B: At. Mol. Opt. Phys.* **30** 4087–96

Nishijima D, Doerner R P, Baldwin M J, De Temmerman G and Hollmann E M 2008 *Plasma Phys. Control. Fusion* **50** 125007
Niyonzima S *et al* 2017 *At. Data Nucl. Data Tables* **115–116** 287–308
Norcross D W and Padial N T 1982 *Phys. Rev.* A **25** 226–338
Pitarch-Ruiz J, Sánchez-Marin J and Velasco A M 2007 *J. Comput. Chem.* **29** 523–32
Pitarch-Ruiz J, Sanchez-Marin J, Velasco A M and Martin I 2008 *J. Chem. Phys.* **129** 054310
Roos J B, Larsson M, Larson A and Orel A E 2009 *Phys. Rev.* A **80** 012501
Samm U 2005 *Nuclear Fusion Research* (Berlin: Springer) pp 3–28
Sanchez I and Martin F 1997 *J. Phys. B: At. Mol. Opt. Phys.* **30** 679–92
Sanna N and Gianturco F A 1998 *Comput. Phys. Commun.* **114** 142–67
Schaftenaar G and Noordik J H 2000 *J. Comput.-Aided Mol. Des.* **14** 123–34
Schumacher U 1983 *Atw. Atomwirtsch. Atomtech.* **28** 500–4
Stibbe D T and Tennyson J 1997 *Phys. Rev. Lett.* **79** 4116–9
Stillinger F H and Herrick D R 1975 *Phys. Rev.* A **11** 446–54
Tarana M, Nestmann B M and Horáček J 2009 *Phys. Rev.* A **79** 012716
Tarana M and Tennyson J 2008 *J. Phys. B: At. Mol. Opt. Phys.* **41** 205204
Tennyson J 1996 *J. Phys. B: At. Mol. Opt. Phys.* **29** 1817–28
Tennyson J 2010 *Phys. Rep.* **491** 29–76
Werner H J *et al* 2008 Molpro, version 2008.1, a package of *ab initio* programs http://molpro.net
Winter H 1975 *Vacuum* **25** 497–511
Yip F L, McCurdy C W and Rescigno T N 2014 *Phys. Rev.* A **90** 063421
Zatsarinny O 2006 *Comput. Phys. Commun.* **174** 273–356
Zatsarinny O and Bartschat K 2004 *J. Phys. B: At. Mol. Opt. Phys.* **37** 2173–89